

# Unfolding of target mass contributions from inclusive proton structure function data

M. E. Christy,<sup>1</sup> J. Blümlein,<sup>2</sup> and H. Böttcher<sup>2</sup>

<sup>1</sup>*Hampton University, Hampton, VA 23668, USA\**

<sup>2</sup>*Deutsches ElektronenSynchrotron, DESY, Platanenallee 6, D15738 Zeuthen, Germany*

(Dated: June 22, 2018)

We report on the extraction of the target mass contributions to the unpolarized proton structure functions by applying an unfolding procedure to the available world data from charged lepton scattering. The method employed is complementary to recent and future parton distribution function fits including target mass contributions and the results obtained can be utilized to further study perturbative QCD at large Bjorken  $x$  and small  $Q^2$ . Global fits are performed to both the available  $F_2^p$  and the separated  $F_L^p$  ( $F_1^p$ ) data which yield excellent descriptions and provides parameterizations of the extracted target mass contributions.

PACS numbers:

## I. INTRODUCTION

Since the inception of QCD as *the* theory of the strong interaction, perturbative QCD (pQCD) has been spectacularly successful in explaining a host of scattering and annihilation processes involving hadrons. Among these is the  $Q^2$  dependence of the proton  $F_2$  structure function measured in charged lepton deeply inelastic scattering (DIS). However, the separation of the *pure* leading twist pQCD  $Q^2$  dependence from possible higher twist (HT) and so called target mass contributions (TMCs) is required for any quantitative study of pQCD at moderate to large values of Bjorken  $x$  and low  $Q^2$ . The large body of existing data on  $F_2^p$  covers a significant range in  $Q^2$  and  $x$ , and is a critical input for pQCD based fits which attempt to extract the parton distribution functions (PDFs). While the contributions from TMCs are now being included in some PDF fits, cf. e.g. [1–5]. Historically the data which were expected to have significant TM or HT contributions were excluded in standard analyses from the fits via kinematic cuts on the invariant hadron mass,  $W$ . Typically, this has removed nearly all the precision data from SLAC at moderate to large  $x$  from the fits, significantly reducing the  $Q^2$  lever arm on the remaining data, and resulting in the rather large error bands quoted from these fits for  $x > 0.5$ .

In this paper we present a fit to the world charged lepton scattering data on the proton  $F_2$  and  $F_L$  ( $F_1$ ) structure functions with the aim of separating the TMCs from the massless limit structure functions via an unfolding procedure. The method employed is complementary to PDF fits including the twist-2 target mass contributions [6], but has the advantage that it does not rely on a finite expansion in the strong coupling constant  $\alpha_s$ . This avoids the issue of disentangling higher order QCD corrections from the TMCs. The extracted distributions still contain the higher twist terms.

## II. DATA SETS

The world charged lepton scattering data sets utilized for the  $F_2$  fit are listed in Table I and include data from the BCDMS [7], and NMC [8] collaborations, the reanalyzed SLAC data from Whitlow *et al.* [9], and the  $e^+$  and  $e^-$  data from the H1 [10, 11] and ZEUS [12, 13] collaborations; the latter two help to constrain the fit at both low  $x$  and large  $Q^2$ . To help constrain the low  $Q^2$  region, recent data from Jefferson Lab Hall C experiments E99-118 [14] and E94-110 [15] have been utilized.

These experiments have additionally performed limited longitudinal and transverse (L/T) separations to extract the information on the transverse structure function,  $F_1$ , the longitudinal structure function,  $F_L$ , and the ratio  $R = F_L/2xF_1$ . For the  $F_L$  fit we include *only* the data extracted via L/T separations in order to minimize the correlation between the  $F_2$  and  $F_L$  data sets. For the JLab experiments, only the L/T separated values for  $F_2$  were utilized. It is unfortunate that more experiments have not made readily available the complete set of separated

---

\*Electronic address: christy@jlab.org

structure functions extracted from L/T separations. Instead, what can generally be found is a table of the extracted  $R = \sigma_L/\sigma_T = F_L/2xF_1$  values, but without the consistently extracted values for  $F_2$  (or  $F_1$ ). In these cases the 'data' on  $F_L$  have been constructed utilizing the available data on  $R$  and a parameterization of the  $F_2$  structure function. The longitudinal structure function was then constructed from

$$F_L = \frac{r^2 F_2}{(1 + R)}, \quad (1)$$

with  $r^2 = 1 + \frac{Q^2}{\nu^2} = 1 + \frac{4M^2 x^2}{Q^2}$ . For this purpose the phenomenological ALLM fit [16] was utilized, which reproduces the world  $F_2$  data to better than 3% and we include this as an additional uncertainty when propagating the uncertainties on  $F_L$  ( $F_1$ ), which are ultimately dominated by the uncertainties on the  $R$  data. The data sets utilized for the  $F_L$  fit are listed in Table II.

Before discussing the procedure, we feel it is worth commenting further on the need for uncorrelated data sets for  $F_L$  and  $F_2$ . This is also important for extractions of PDFs utilizing pQCD fits, since  $F_L$  provides direct information on the gluon content that is only present in  $F_2$  through the shallow logarithmic scaling violations. In principle, the most information on the structure can be obtained from the full data set on the reduced cross section, which is proportional to  $r^2 F_2 - (1 - \epsilon)F_L(x, Q^2)$ , with  $\epsilon$  a kinematic factor describing the photon polarization. Most of the DIS data sets extract  $F_2$  utilizing *all* the cross section measurements, after first determining  $R$  by a linear fit in  $\epsilon$  to the reduced cross section measurements at different  $\epsilon$  values at fixed  $x$  and  $Q^2$  (the Rosenbluth separation technique [17]).

### III. PROCEDURE

We follow the formalism for including TMCs to the massless limit structure function developed by Georgi and Politzer [6] within the operator product expansion (OPE). This approach was extended by Kretzer and Reno [18] to include the full set of electro-weak structure functions using modern formalism. For a recent review of TMCs see [19].

At fixed  $Q^2$  the  $F_2$  structure function, including TM effects, can be written

$$F_2^{TM}(x, Q^2) = \frac{x^2 F_2^{(0)}(\xi, Q^2)}{r^3 \xi^2} + 6 \frac{M^2 x^3}{Q^2 r^4} \int_{\xi}^1 dx' \frac{F_2^{(0)}(x', Q^2)}{x'^2} + 12 \frac{M^4 x^4}{Q^4 r^5} \int_{\xi}^1 dx' \int_{x'}^1 dx'' \frac{F_2^{(0)}(x'', Q^2)}{x''^2} \quad (2)$$

Here,  $F_2^{(0)}(x, Q^2)$  is the massless limit structure function which can be calculated in pQCD utilizing the PDFs determined at some scale,  $\xi = 2x/(1+r)$  is the Nachtmann scaling variable, and both  $x'$  and  $x''$  are dummy integration variables. The corresponding TMC equation for  $F_L$  is

$$F_L^{TM}(x, Q^2) = \frac{x^2 F_L^{(0)}(\xi, Q^2)}{r \xi^2} + \frac{4M^2 x^3}{Q^2 r^2} \int_{\xi}^1 dx' \frac{F_2^{(0)}(x', Q^2)}{x'^2} + \frac{8M^4 x^4}{Q^4 r^3} \int_{\xi}^1 dx' \int_{x'}^1 dx'' \frac{F_2^{(0)}(x'', Q^2)}{x''^2}. \quad (3)$$

The transverse structure function including the TM contributions, can then be constructed from

$$2xF_1^{TM} = \frac{F_2^{TM} - F_L^{TM}}{r^2} \quad (4)$$

and in the massless limit ( $r \rightarrow 0$ ) from

$$2xF_1^{(0)} = F_2^{(0)} - F_L^{(0)}. \quad (5)$$

We note that these equations are valid to all orders in pQCD at twist 2. The target mass corrections for higher twist operators in the unpolarized case are yet unknown. Moreover, dynamical higher twist contributions, starting with twist 4, cannot be described with one scaling variable only, neither do their potential target mass corrections, because the main variable  $x$  is supplemented by further other invariants  $x_i$ . Their number grows with the level of twist included. This implies the necessity to study different multi-parton correlations, which cannot be determined by inclusive measurements as that of the deep-inelastic structure functions only. Because of this the present analysis remains phenomenological applying the twist 2 target mass corrections to the structure functions. [30]

While it is  $F_2^{TM}(x, Q^2)$  that is measured in scattering experiments, it is the  $Q^2$  evolution of  $F_2^{(0)}$  that is described by pQCD. To extract  $F_2^{(0)}$  from data requires the inversion of Eq. (2). The procedure for extracting the TM corrected

$F_2$  structure function is to parameterize  $F_2^{(0)}(x, Q^2)$  and then to minimize the  $\chi^2$  difference between the left-hand side of Eq (2) and the  $F_2$  data:

$$\chi^2 = \Sigma \left( \frac{F_2^{TM} - F_2^i}{\delta F_2^i} \right)^2, \quad (6)$$

where  $F_2^i$  is the value of the  $i^{th}$  data point and  $\delta F_2^i$  it's uncorrelated uncertainty.

TABLE I: Data sets used in  $F_2$  fit.

Data Set	$Q_{Min}^2$ (GeV <sup>2</sup> )	$x_{min}$	$Q_{Max}^2$ (GeV <sup>2</sup> )	$x_{max}$	# Data Points
BCDMS [7]	7.5	0.070	230	0.75	178
NMC [8]	0.75	0.0045	65	0.50	158
SLAC (Whitlow [9])	0.58	0.063	30	0.90	661
H1 [10, 11]	1.5	$3.0 \times 10^{-5}$	5000	0.32	286
Zeus [12, 13]	3.5	$6.3 \times 10^{-5}$	5000	0.20	228
E99-118 [14]	0.273	0.077	1.67	0.320	9
E94-110 [15]	0.7	0.19	3.5	0.57	12

TABLE II: Data sets used in  $F_L$  ( $F_1$ ) fit.

Data Set	$Q_{Min}^2$ (GeV <sup>2</sup> )	$x_{min}$	$Q_{Max}^2$ (GeV <sup>2</sup> )	$x_{max}$	# Data Points
BCDMS [7]	15	0.07	50	0.65	10
EMC [21]	15	0.041	90	0.369	28
NMC [8]	1.31	0.0045	20.6	0.11	10
SLAC (Whitlow [22])	0.63	0.1	20	0.86	90
SLAC (E140x [23])	0.5	0.1	3.6	0.50	4
H1 [24]	1.5	$3.0 \times 10^{-5}$	45	0.0015	13
ZEUS [25]	24	$6.7 \times 10^{-4}$	110	0.0049	18
E99-118 [26]	0.273	0.077	1.67	0.320	8
E94-110 [15]	0.7	0.19	3.5	0.57	12

The fit form utilized for the  $x$  dependence of both  $F_2^{(0)}$  and  $F_L^{(0)}$  was

$$F_{2,L}^{(0)}(x) = Ax^B(1-x)^C(1 + D\sqrt{x} + Ex), \quad (7)$$

with the  $Q^2$  dependence of A, B, C, D, and E parameterized as

$$A(Q^2) = A_1 + A_2 e^{-Q^2/A_3} + A_4 \log(0.3^2 + Q^2). \quad (8)$$

These forms are empirical, but were found to give a good description of the data. The fitting was performed utilizing MINUIT [27] and utilized an optimized FORTRAN routine DAIND [29] to perform the single and double integrations in Eqs. (2) and (3).

#### IV. RESULTS AND CONCLUSIONS

The fit results for both  $F_2$  and  $F_L$  are quite good, with  $\chi^2$  per degree of freedom ( $\chi^2/\text{DoF}$ ) of 1.01 and 0.93 for  $F_2$  and  $F_L$ , respectively. The resulting fit parameters are listed in Table III for  $F_2$  and Table IV for  $F_L$ . Comparisons of the fit results to the  $F_2$  data are shown in Figure 1 for the 6 different  $Q^2$  values listed on the panels from 1 to 100 GeV<sup>2</sup>. Data within a range of  $Q^2$  about the central value have been centered to the common  $Q^2$  value using the fit. A comparison over the full  $x$  range fit is shown (Left), as well as for large  $x$  (Right). Similar comparisons for  $F_L$  are shown in Figure 2. Of particular note is the lack of quality data for  $F_L$  in the range  $0.005 < x < 0.3$  for

TABLE III:  $F_2$  best fit parameters.

$n =$	1	2	3	4
$A_n^2$	0.2145	0	0	0
$B_n^2$	-2.1540	.0808	5.6730	-0.0319
$C_n^2$	2.7830	-0.5013	7.104	0.1857
$D_n^2$	-0.8997	-3.1092	0.3820	-0.1275
$E_n^2$	9.0441	0	0	0

TABLE IV:  $F_L$  best fit parameters. Parameter  $C_1^L$  (indicated by \*) has been fixed, as the goodness of the fit was found to be only minimally sensitive to it's value.

$n =$	1	2	3	4
$A_n^L$	0.0078	0.0	0.0	0.0
$B_n^L$	-2.0650	0.0	0.0	-4.8846
$C_n^L$	1.0*	0.0	0.0	0.0
$D_n^L$	0.0	-0.0030	0.0	0.6040
$E_n^L$	0.0	0.0	0.0	0.0

$Q^2 > 3 \text{ GeV}^2$ . Such data is critical for constraining the fit at low  $x$  and would be of particular value in constraining the gluon distribution which is a dominant contribution to  $F_L$ .

We expect that the fit will be of interest to the broader community in providing a good description of the data on the full set of unpolarized structure functions in charged lepton scattering from the proton,  $F_2$ ,  $F_L$ ,  $F_1$ , and  $R$ , over the kinematic range of  $x > 3 \times 10^{-5}$  and  $0.1 < Q^2 \text{ GeV}^2$ , in addition to providing a separation of the TMCs from the massless limit structure functions.

The separated structure functions can be used for further pQCD studies, such as HT analyses of both the structure functions and moments. The current analysis procedure is complementary to PDF fits which include TMCs in that the unfolding of the TMCs does not depend on a finite order expansion in  $\alpha_S$ . Comparison of the results from the two procedures could provide an additional handle on isolating HT contributions from higher-order QCD corrections and making for a 'cleaner' evaluation of the former.

Additionally, the fit will be of use in future studies of quark-hadron duality. In particular, determining how well the *averaged* resonance region structure functions at fixed  $x$  obey the  $Q^2$  dependence dictated from DIS.

FORTTRAN computer code embodying the fit described in this article is available by email request from the authors, including the full covariance matrices.

### Acknowledgments

We would like to thank R. Ent, C.E. Keppel, and A. Accardi for useful discussions. This work was supported in part by research grant 1002644 from the National Science Foundation and by the Deutsche Forschungsgemeinschaft in Sonderforschungsbereich/Transregio 9 and by the European Commission through contract PITN-GA-2010-264564 (LHCPhenoNet).

- 
- [1] S. I. Alekhin, Phys.Rev. **D63**, 094022 (2001), hep-ph/0011002.
  - [2] J. Blümlein, H. Böttcher, and A. Guffanti, Nucl.Phys.Proc.Suppl. **135**, 152 (2004), hep-ph/0407089.
  - [3] J. Blümlein, H. Böttcher, and A. Guffanti, Nucl.Phys. **B774**, 182 (2007), hep-ph/0607200.
  - [4] S. Alekhin, J. Blümlein, S. Klein, and S. Moch, Phys. Rev. D **81**, 014032 (2010).
  - [5] A. Accardi et al., Phys. Rev. D **81**, 034016 (2010).
  - [6] H. Georgi and H. D. Politzer, Phys. Rev. D **14**, 1829 (1976).
  - [7] A. Benvenuti et al., Phys. Lett. B **237**, 592 (1990).
  - [8] M. Arneodo et al., Nucl. Phys. B. **483**, 3 (1997).
  - [9] L. W. Whitlow et al., Phys. Lett. B **282**, 475 (1992).

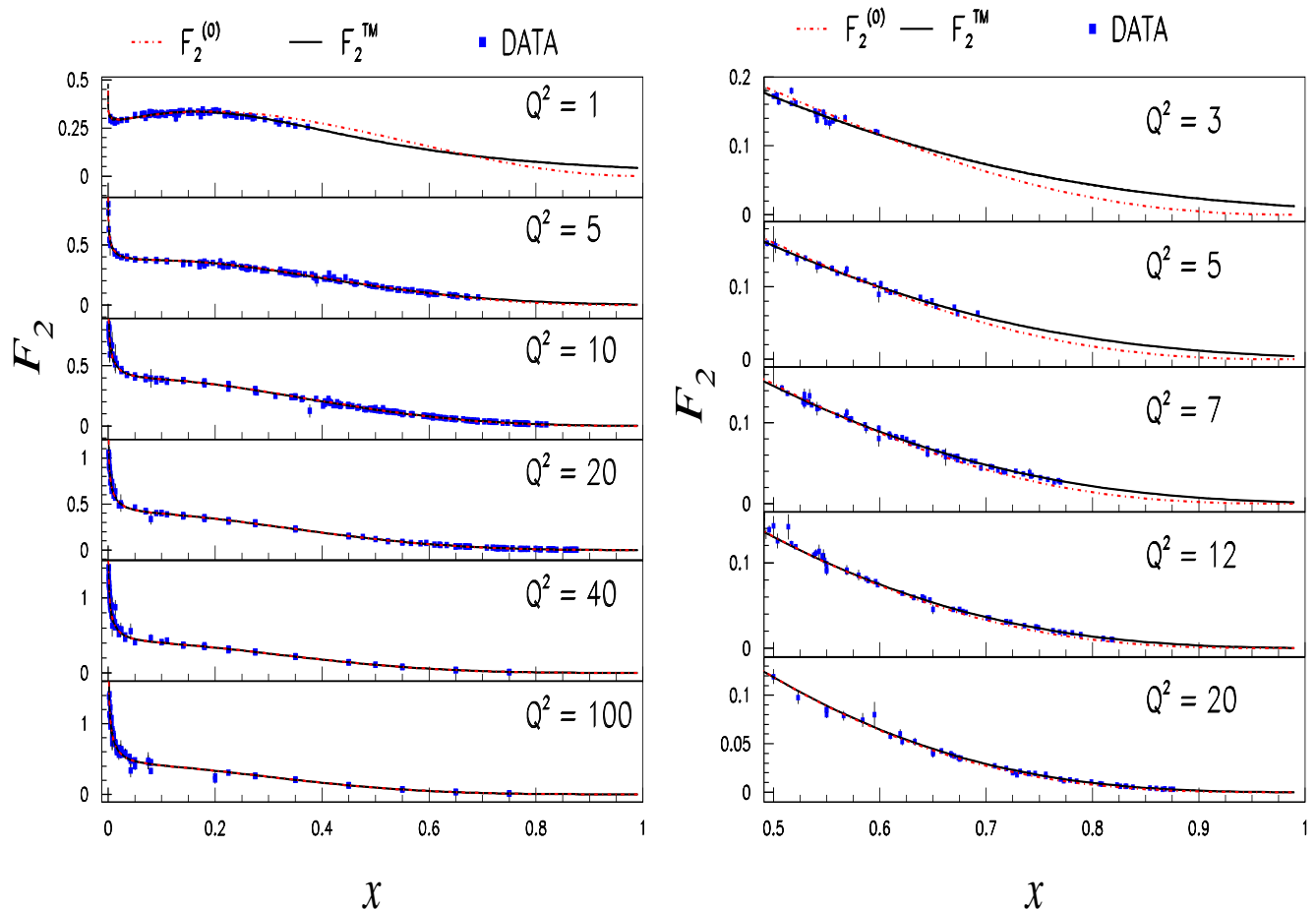


FIG. 1: (Color online) Comparison of the  $F_2^{TM}$  fit results (dashed curve) to the proton data for 6 different  $Q^2$  values (left panel). The low  $x$  data from H1 and ZEUS are beyond the vertical scale. Also shown is the massless limit structure function parameterization from the fit (solid curve). A zoom view for the region  $x > 0.5$  is also shown for 5 different  $Q^2$  values (right panel).

- [10] T. Ahmed et al., Nucl. Phys. B **470**, 3 (1996).
- [11] T. Ahmed et al., Nucl. Phys. B **439**, 471 (1995).
- [12] M. Derrick et al., Zeit. Phys. C **65**, 379 (1995).
- [13] M. Derrick et al., Zeit. Phys. C **72**, 399 (1996).
- [14] V. Tvaskis et al., Phys. Rev. C **81**, 055207 (2010).
- [15] Y. Liang et al. (2004), nucl-ex/0410027.
- [16] H. Abramowicz and A. Levy (1997), hep-ph/9712415.
- [17] M. N. Rosenbluth, Phys. Rev. **79**, 615 (1956).
- [18] S. Kretzer and M. Reno, Phys. Rev. D **69**, 034002 (2004).
- [19] I. Schienbein et al., J. Phys. G **35**, 053101 (2008).
- [20] Note1, in Ref. [28] also the fermionic twist-3 target mass corrections in case of polarized deep-inelastic scattering have been calculated. They operate on the structure functions similar to the case of the twist-2 corrections as long as no gluonic operators in the respective region, i.e. at large  $x$ , are relevant. The polarized twist-3 TMCs are described by different integrals as those at twist 2. However, quantitative numerical case studies using the same shape for input distributions have not been performed yet.
- [21] J. Aubert et al., Nucl. Phys. B **259**, 189 (1985).
- [22] L. W. Whitlow et al., Phys. Lett. B **250**, 193 (1990).
- [23] L. H. Tao et al., Z. Phys. C **70**, 387 (1996).
- [24] F. Aaron et al., Eur. Phys. J. C **71**, 1579 (2011).
- [25] S. Chekanov et al., Phys. Lett. B **682**, 8 (2009).
- [26] V. Tvaskis et al., Phys. Rev. Lett. **98**, 142301 (2007).

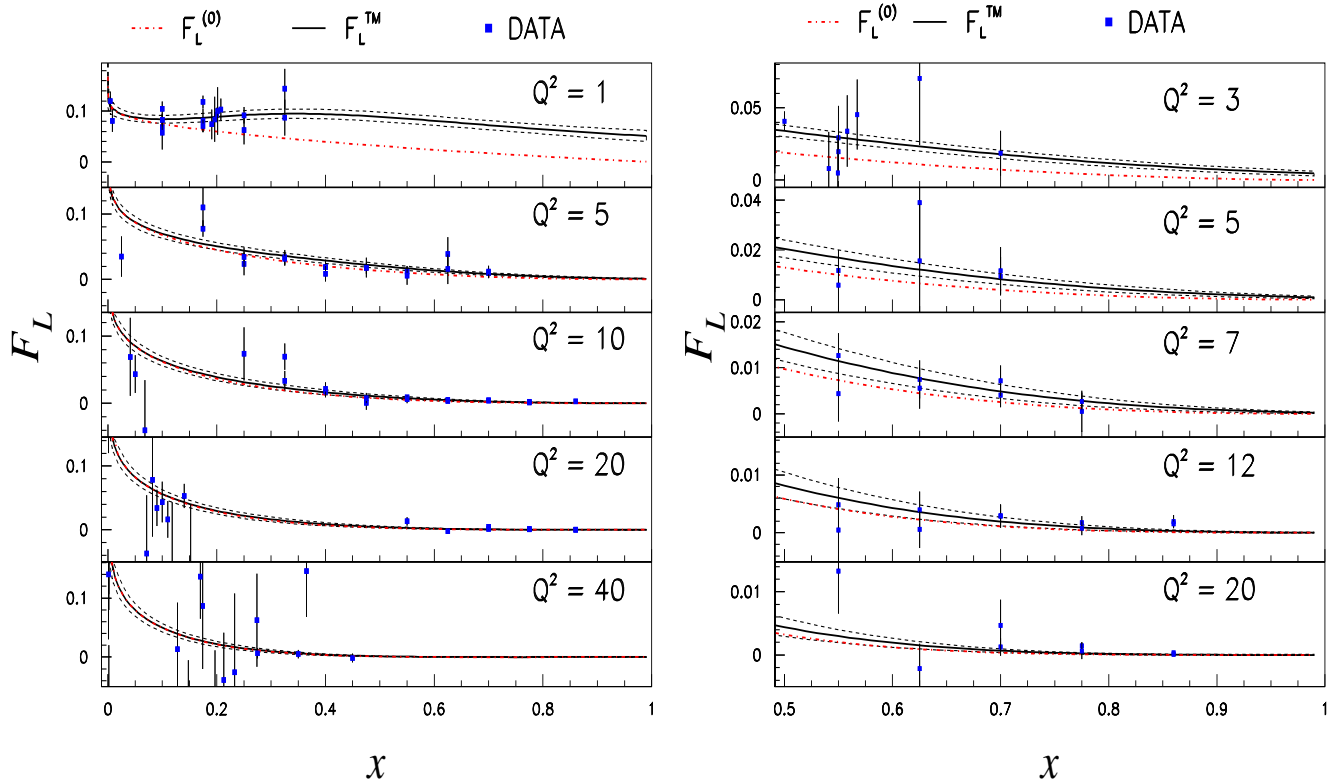


FIG. 2: (Color online) Comparison of the  $F_L^{TM}$  fit results (solid curve) to the proton data versus  $x$  for 5 different  $Q^2$  values (left panel). The low  $x$  data from H1 and ZEUS are beyond the vertical scale. Also shown is the massless limit structure function parameterization from the fit (dot-dashed curve). A zoom view for the region  $x > 0.5$  is also shown (right panel). All data within a range of  $\pm 40\%$  ( $Q^2 = 1$ ),  $\pm 33\%$  ( $Q^2 = 3$ ),  $\pm 15\%$  ( $Q^2 = 5, 7, 10,$  and  $12$ ), and  $\pm 20\%$  ( $Q^2 = 20$  and  $40$ ) have been bin-centered to the central  $Q^2$  using the  $Q^2$  dependence from the fit. The uncertainty band stemming from the uncorrelated uncertainties and calculated from the fit covariance matrix is indicated by the dashed curve.

[27] F. James, MINUIT Reference Manual, CERN Program Library Writeup, D506 (1998).

[28] J. Blümlein and A. Tkabladze, Nucl.Phys. **B553**, 427 (1999), hep-ph/9812478.

[29] R. Piessens, Angew. Informatik **9**, 399 (1973).

[30] In Ref. [28] also the fermionic twist-3 target mass corrections in case of polarized deep-inelastic scattering have been calculated. They operate on the structure functions similar to the case of the twist-2 corrections as long as no gluonic operators in the respective region, i.e. at large  $x$ , are relevant. The polarized twist-3 TMCs are described by different integrals as those at twist 2. However, quantitative numerical case studies using the same shape for input distributions have not been performed yet.